EPI distortion correction using highly under-sampled point-spread function estimation based on Finite Rate of Innovation

Rita G. Nunes[1,2] and Joseph V. Hajnal[2,3]

[1]*Institute of Biophysics and Biomedical Engineering, Faculty of Sciences, University of Lisbon, Lisbon, Portugal,* [2]*Division of Imaging Sciences and Biomedical Engineering, King's College London, London, United Kingdom,* [3]*Centre for the Developing Brain, King's College London, London, United Kingdom*

Target audience: People using Echo-planar Images, particularly if acquired at high magnetic fields (3.0T and higher), who wish to correct for geometric distortions.

Purpose: Echo-planar images (EPI) present geometric distortions due to static B0 field inhomogeneities. Several approaches have been developed for correction including direct B0 [1] and Point Spread Function (PSF) mapping [2]. To measure the PSF, an extra encoding gradient (G_s) is added in the phase encode direction prior to the EPI readout. This gradient is associated with another k-space (k_s) which spatially encodes the PSF along undistorted spatial coordinates s. To map the PSF, the standard EPI sequence is repeated while incrementing G_s, allowing sampling of k_s. Although PSF correction has been shown to be more robust compared to B0 mapping [3], long acquisition times have limited its application. Previous approaches to accelerate PSF mapping include Parallel Imaging (PPI) [4], reduced field of view (rFOV) acquisitions [5,6], or using a Dictionary Learning compressed sensing framework to recover the full PSF shape [7]. Even when achieving high acceleration factors (10 or more), a minimum number of 10 PSF phase encoding samples was required, despite the fact that most PSF distortion correction schemes take into account only the position of the PSF peak. If only this information is required and the PSF can be described by a dominant peak in s-space, then the Finite Rate of Innovation framework [8,9] should be applicable. Signals with a finite rate of innovation typically have only a number of discrete events within a given measurement interval. In this case there is one event, the PSF within the FOV. We therefore seek a single delta function that matches the peak location and aim to determine its position to sub-pixel precision using as few k_s samples as possible.

$$Ncc(s) = \sum_{k_s samples} \frac{Sig(r,k_s).f(s,k_s)}{\sqrt{cc_{Sig}\,cc_f}}$$

Equation 1: Normalized Cross-Correlation, where cc_{Sig} and cc_f representing the auto-correlation functions for $Sig(\mathbf{r},k_s)$ and $f(s,k_s)$.

Theory: To determine the position of the PSF peak, pattern matching is performed. Taking into account the employed k_s sampling scheme, the measured signal $Sig(\mathbf{r},k_s)$ at each spatial location **r** is compared to a predicted signal pattern $f(s,k_s)=\exp(i2\pi s k_s)$ (corresponding to a delta function centered at s in the PSF spatial domain) by calculating their normalised cross correlation, Ncc (Equation 1). Using a simple search strategy the PSF peak location is identified by maximising Ncc(s). Initially a set of candidate s are evaluated in integer pixel units. The search is then progressively refined by defining new sets of s centred on the last estimated location but at finer spacing. The number of iterations is set by the intended precision.

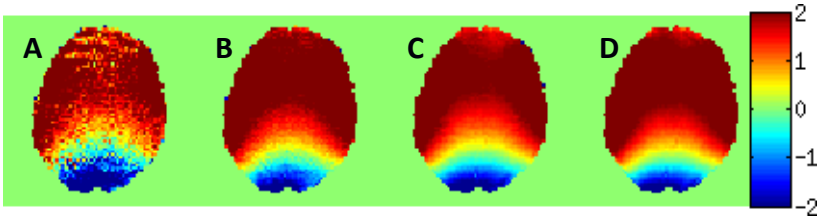

Figure 1: Maps of the PSF shifts (in pixels) estimated with: **A)** 2; **B)** 3; **C)** 4; **D)** all 95 k_s.

Methods: Images were acquired on three volunteers on a 3.0T Philips Achieva. Image resolution 2.5×2.5×4.0 mm^3, matrix 96×95, 95 PSF encoding steps (PSF and EPI with matched FOVs), 24 slices, TE/TR = 35/3000 ms. An EPI image was reconstructed using the non-PSF encoded repeat, while a gradient echo (GE) image was obtained by taking all central lines of the EPI readout. Under-sampling was retrospectively performed along the PSF encoding direction using just 2-4 samples, with the sampling locations selected following a Monte Carlo simulation study: 2 samples (k_s=0, 1 Δk_s), 3 samples (k_s= 0, 1, 4 Δk_s), 4 samples (k_s= 0, 5, 13, 25 Δk_s), where Δk_s is the k_s step size used in the acquisition. For each voxel in the images, the position of the PSF peak was estimated using both the fully-sampled and highly-undersampled data. The fully-sampled data was zero-filled by a factor of 1000, and the PSF peak determined in image-space to a precision of 0.001 pixel units. To undistort the EPI images, the procedure described in [10] was performed.

# k_s samples	2	3	4
abs. error (%)	2.8 1.6- 4.5	0.97 0.71-1.20	0.5 0.43 – 0.54

Table 1 – Absolute relative errors for the PSF peak position estimated with under-sampled data compared to fully-sampled acquisition (median over brain pixels). Mean value and range observed for the three subjects.

Results: Example maps of the estimated PSF peak shifts (relative to the expected undistorted positions) are shown in Figure 1 for all tested sampling schemes. The median absolute relative errors over the whole brain were quantified using the fully-sampled data as reference – Table 1. Figure 2A shows the original EPI slice matching Figure 1, and Figures 2B-E show the corrected images using each displacement map. Comparison with the GE image (Figure 2F) confirms that accurate geometrical corrections were achieved in each case.

Discussion and Conclusions: Using the proposed approach it is possible to estimate the position of the PSF peak from a very small number of PSF samples (one of which can be acquired at k_s=0 corresponding to the standard EPI acquisition). The implication is that, in the future, distortion map estimation using the PSF method could easily be incorporated into standard preparation phases.

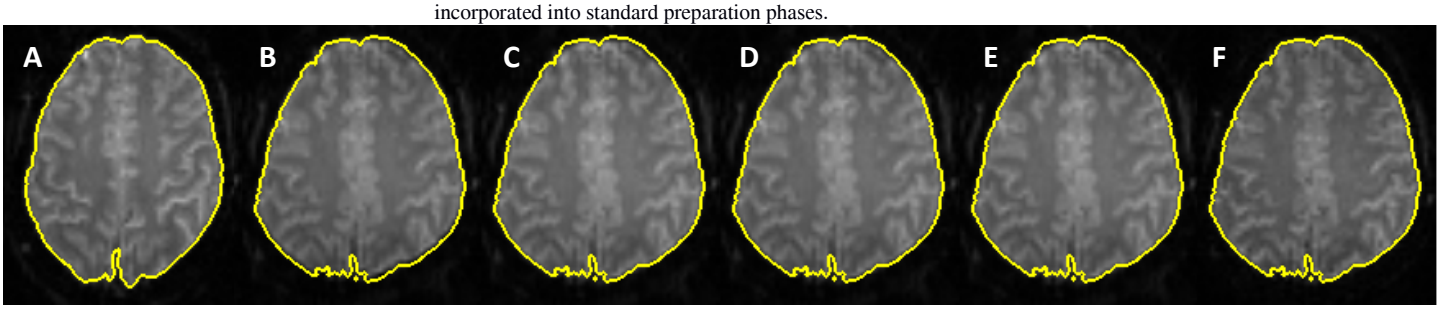

Figure 2: A) EPI image (with corresponding outer contour in yellow); Undistorted EPI images estimating the displacement field from: **B)** 2; C) 3; **D)** 4 and **E)** all 95 k_s samples and **F)** GE image (corresponding outer contour in yellow propagated to all undistorted EPI images).

References: [1] Jezzard P et al, MRM, 1995, 34:65; [2] Robson MD et al, MRM, 1997, 38:733. [3] Zeng H et al, MRM, 2002, 48:137. [4] Zaitsev M et al, MRM, 2004, 52:1156; [5] In M et al, MagnResonMaterPhy, 2012, 25:183; [6] Dragonu I et al, MRM, 2013, 69:1650; [7] Nunes RG et al, ESMRMB, 2013, 30:145; [8] Vetterli M et al, IEEE Trans Sig Process, 2002, 50:1417; [9] Maravic I et al, IEEE Trans Sig Process, 2005, 53:2788; [10] Oh SH et al, MRM, 2012, 68:1239.